JOURNAL OF CATALYSIS 149, 181–188 (1994)

On the Acid-Catalyzed Isomerization of Light Paraffins over a ZrO_2/SO_4 System: The Effect of Hydration

C. Morterra,*,[1] G. Cerrato,* F. Pinna,† M. Signoretto,† and G. Strukul†

*Department of Inorganic, Physical, and Materials Chemistry, University of Turin, Via P. Giuniat, I-10125 Turin, Italy; and †Department of Chemistry, University of Venice, Calle Larga St. Marta 2137, I-30123 Venice, Italy

Received December 20, 1993; revised March 9, 1994

Over a superacid ZrO_2/SO_4 system (ZS8: microcrystalline tetragonal, SO_4 content ≈2.6 groups per nm^2), the isomerization of *n*-butane proceeds rapidly and with high yield of i-butane at 423 K, if the catalyst is calcined in dry air at ≈823 K. The active catalyst typically shows: all surface sulfates in a highly covalent form, a high concentration of strong (aprotic) Lewis acid sites, and a fairly low (though never null) concentration of (protonic) Brønsted acid sites. A partial rehydration of the catalyst gradually converts the surface sulfates first into a less covalent form and then into an ionic form, decreases the concentration of strong Lewis sites, and increases (up to a factor of ≈10) the concentration of Brønsted sites, while the catalytic activity is gradually extinguished. Initial activity and initial surface features can be recovered by repeating the catalyst activation step. © 1994 Academic Press, Inc.

1. INTRODUCTION

The isomerization reaction of light paraffins, leading to the formation of branched isomers, is an important process in the petroleum refining industry. This reaction is known to be acid-catalyzed and to require very strong acid sites. It is also known that solid superacids, obtained by doping ZrO_2 (and other oxides) with appropriate amounts of sulfate groups, can promote various catalytic processes (including, for instance, the isomerization of light paraffins) that do not occur with appreciable yield on the pure oxides. Despite a significant number of papers dealing with this subject (e.g., see (1–3), and references therein), the exact nature of the active sites on sulfate-doped systems is still not clearly established. In particular, the role played by Lewis (aprotic) and Brønsted (protonic) acid centres is still controversial.

Many preparative parameters have been observed to affect nature and strength of the active sites on sulfate-doped ZrO_2, and quite important among them seem to be: ZrO_2 preparation procedure, ZrO_2 prefiring temperature, sulfate-doping procedure, sulfate loading, and the temperature of catalyst calcination (activation) before reaction.

As for the role played by the hydration/dehydration stage reached by the catalyst before reaction, contradictory data are available in the literature. Tanabe *et al.* (4) report that, when exposed to the air at ambient temperature, solid superacids lose their superacidic activity by absorbing moisture. Parera (5) reported that the partial rehydration of superacid catalysts with air saturated with water vapour, with consequent regeneration of some OH groups and the possible transformation of some Lewis sites into Brønsted sites, does not affect the catalytic activity in the isomerization reaction of *n*-butane. Wen *et al.* (6) found that the presence of small amounts of moisture in the reaction system enhances the catalytic activity of a platinum-doped solid superacid ($Pt/ZrO_2/SO_4$) in the hydroisomerization and hydrocracking of *n*-heptane, probably due to the transformation of Lewis sites into Brønsted sites.

We have recently started a systematic characterization of some sulfate-doped zirconia catalysts, prepared by impregnating amorphous $Zr(OH)_4$ with $(NH_4)_2SO_4$ (7). In particular, the particles texture and some of the surface features of the catalytic systems have been related to the catalytic activity towards *n*-butane isomerization.

In the present contribution we report in some detail the influence of H_2O addition on the catalyst activity, and the parallel modification brought about by H_2O addition in the surface features of the ZrO_2/SO_4 system.

2. EXPERIMENTAL

2.1. Materials

$Zr(OH)_4$ was prepared by the sol–gel technique, by adding a mixture of isopropyl alcohol (30 ml) and water (4 ml) to a solution of Zr propoxide (18 ml) in isopropyl alcohol (60 ml), containing HNO_3 (65%, 0.6 ml) as a catalyst. This solution was kept under continuous stirring for 30 min at 298 K and then aged for 24 h at 313 K in order to complete the polycondensation reaction; the gels so obtained were then dried at 423 K very slowly. Under these conditions, the zirconia obtained is highly hydrated

[1] To whom correspondence should be addressed.

0021-9517/94 $6.00

and amorphous. The IR spectrum shows strong broad absorptions in the 1700–1000 cm^{-1} range, due to adsorbed water, carbonate-like species (due to CO_2 uptake from the atmosphere) and, possibly, traces of nitrates. (It is known that surface nitrates are hardly distinguishable from surface carbonates). All these species are at the surface of the bulky $Zr(OH)_4$, as they are eliminated when a thermal treatment is carried out in dry air or *in vacuo* at $T \geq 693$ K, leading to microcrystalline mixed tetragonal–monoclinic ZrO_2.

For the sulfation, $Zr(OH)_4$ (10 g) was suspended into an aqueous solution of $(NH_4)_2SO_4$ (1 *M*, 9 ml). The mixture was stirred for 2 h, slowly evaporated to dryness, and finally calcinated in dry air for 3 h at $T_1 \geq 673$ K. Typically, the BET surface area of the sulfated samples was 235 $m^2 g^{-1}$ for $T_1 = 673$ K, 188 $m^2 g^{-1}$ for $T_1 = 823$ K, and 132 $m^2 g^{-1}$ for $T_1 = 923$ K.

No trace of carbonates and/or nitrates remains in the IR spectrum of the sulfated ZrO_2 specimens after the calcination stage. This implies that, if carbonates and/or nitrates were present in the starting hydroxide, they were eliminated during the sulfation/calcination steps, and that after sulfation (i.e., in the presence of surface sulfates) no basic sites remain at the surface of the material for the formation of carbonates from atmospheric CO_2.

The ZrO_2/SO_4 system is designated in the text and figures by the symbol ZS8(T_1)T_2. T_1 is the calcination temperature, i.e., the temperature (K) at which the catalyst was first fired in a dry air stream. T_2 is the activation temperature, i.e., the temperature (K) at which each sample was thermally treated for 2 h in dry air (for the catalytic tests), or *in vacuo* (for the IR experiments), before undergoing the catalytic tests or *in situ* IR determinations.

The concentration of sulfates at the surface of ZS8(T_1) systems, with $773 \leq T_1 \leq 973$ K (i.e., of the ZS8 systems that are catalytically active, as reported below), was determined with a chemical analytical technique to be described elsewhere. For $T_1 = 823$ K, the nominal concentration of sulfates, calculated assuming that the amount of sulfates absorbed initially on the amorphous hydroxide is all present (only) at the surface, is $\approx$2.6 SO_4 groups per nm^2 (it is here recalled that a nominal monolayer of SO_4 contains a maximum of four groups per nm^2 (2)). For $T_1 = 823$ K, the chemical analysis yields a concentration of 2.6 $\pm$ 0.1 sulfate groups per nm^2. For $T_1 = 923$ K (the catalyst is still active) the sulfate concentration becomes 1.5 $\pm$ 0.1 groups per nm^2, and then declines rapidly for $T_1 \geq 973$ K, when the thermal decomposition of sulfates becomes abundant.

2.2. Methods

The isomerization reaction was performed in a continuous flow reactor made from a quartz glass tube (i.d. = 8 mm) heated by an external oven. A small glass tube containing an Fe–Ko thermocouple was placed in the middle of the catalyst bed. The system was operated in the following conditions: reaction temperature, 423 K; total gas pressure, 1 atm; *n*-butane : helium ratio = 3 : 1; space velocity, 200 h^{-1}. Prior to reaction, the catalyst (1.5 g, 100–120 mesh) was treated in a dry air stream at the chosen temperature T_2 for 2 h (activation stage), and then cooled to the reaction temperature (423 K). Before entering the reactor, the feed stream was preheated at 423 K. All reactant and product gas concentrations were measured on line by gas chromatography.

To test the effect of hydration, different doses of H_2O (1.5, 3.7, 7.4, and 11.1 μl) were introduced through a vaporizer (423 K) into the reactants with a microsyringe.

All the samples used for IR measurements were in the form of thin-layer depositions, obtained by spreading an aqueous suspension of the catalyst over a pure Si platelet. This sample preparation procedure was necessary because the usual self-supporting pellets, employed routinely in the spectroscopic study of adsorbed species, are optically too thick for the observation of the surface sulfates absorbing strongly at $\nu < 1500$ cm^{-1}. The dried depositions were transferred to a conventional quartz cell, where the samples underwent all thermal and adsorption treatments as described below. FTIR spectra were run at 2 cm^{-1} resolution with a Bruker 113v spectrophotometer equipped with MCT detector. The dosing and evacuation of gases was carried out using a strictly *in situ* configuration, that allowed reliable background subtractions.

(HR) TEM micrographs were obtained with a Jeol JEM 2000 EX electron microscope, equipped with a top-entry stage; the samples were deposited from *n*-heptane dispersions on Cu grids, coated with a holey carbon film.

XRD data were obtained with a Philips PW 1830 diffractometer (Co$K\alpha$).

3. RESULTS AND DISCUSSION

3.1. Catalytic Activity

For calcination at $T_1 = 673$ K, when the system starts crystallizing, the catalytic activity of ZS8 for *n*-butane isomerization is null, and is still virtually null for $T_1 = 773$ K (7). This confirms that the preparation conditions are crucial in determining the catalytic properties of ZrO_2/SO_4 systems (1, 8). For $T_1 = 823$ K, when the concentration of sulfates is maximum, the catalytic activity of the ZS8 system is high. In this stage, the ZrO_2/SO_4 system is made up of large aggregates (50–100 nm size) of tiny microcrystalline particles (3–10 nm), flat and irregularly shaped, belonging entirely to the tetragonal form, as shown by the X-ray diffraction pattern and the high resolution transmission electron micrograph reported in Fig. 1.

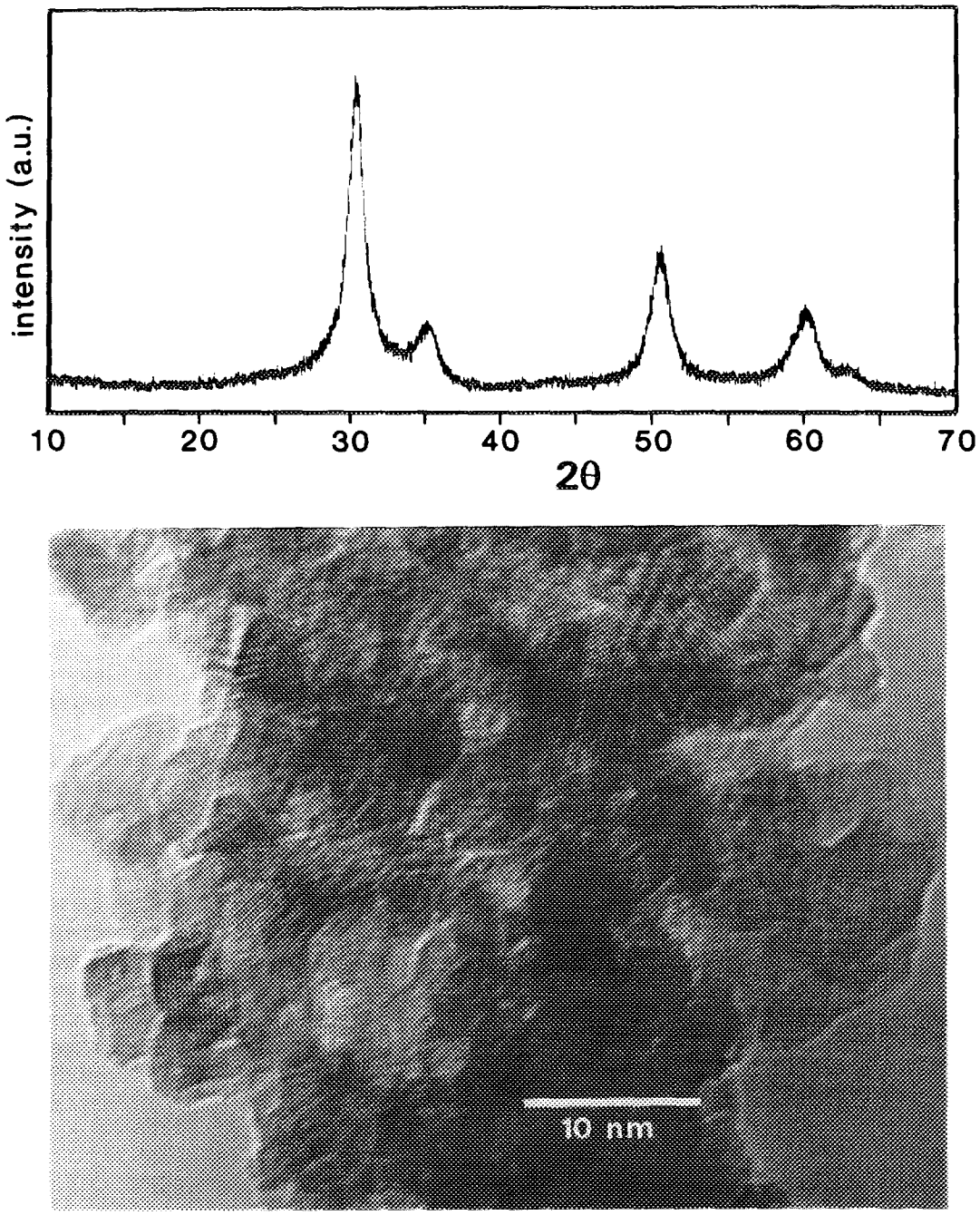

FIG. 1. Segment of the XRD pattern (upper section) and HRTEM image (lower section) of the ZS8(823) sample.

Figure 2 reports the catalytic activity of some ZS8(823)723 samples. The activity is defined as the total conversion of *n*-butane as a function of the time on stream, when dry air is replaced in the reactor by a mixture of *n*-butane and dry helium. At the beginning of the run a fast decrease of activity is observed. Besides i-butane, small amounts of methane and propane are detected, indicating some activity of the fresh catalyst also towards cracking and disproportionation reactions.

After ≈30 min in stream the conversion practically reaches a steady state. The selectivity towards i-butane is extremely high (about 98%), probably because, once formed, i-butane desorbs from the acid sites before reaching the equilibrium.

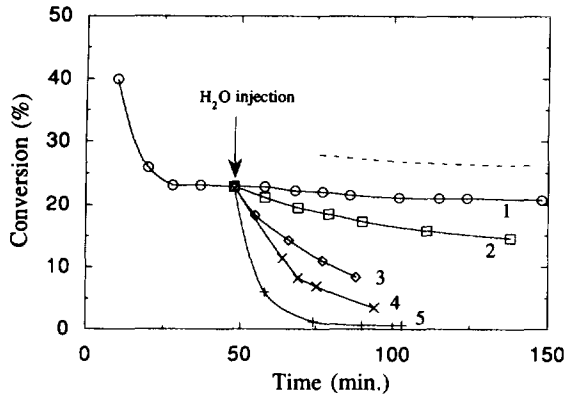

FIG. 2. Catalytic conversion of *n*-butane as a function of time on stream for ZS8(823)723 (curve 1) and for ZS8(823)873 (dashed-line trace). Curves 2–5 show the effect of water addition on the conversion over the ZS8(823)723 sample. The nominal fractions of surface reacted with H_2O are: (2) 10%, (3) 25%, (4) 50%, and (5) 75%.

It is important to note that, whenever the activity of an aged catalyst declines, the initial catalytic activity can be completely recovered by repeating the activation stage, i.e., by reactivating the catalyst in dry air at T_2 = 723 K.

To test the effect of H_2O addition on the catalytic activity, a series of consecutive runs have been performed by injecting variable amounts of H_2O (as indicated in the Experimental section), after 50 min on stream. H_2O doses were chosen so as to interact with a predetermined percentage of the exposed catalyst surface, and/or with a predetermined fraction of the sulfur surface content, on the assumption that H_2O is readily and competitively adsorbed at the surface of SO_4/ZrO_2 systems. This assumption is confirmed by independent IR data.

The effect of the various water additions on the working catalyst is shown by the numbered lines in Fig. 2. After each run the catalyst was reactivated, and a new water dose was injected into the reacting system.

For the sake of simplicity, the conversion up to 50 min for the runs 2–5 is not reported in the plot of Fig. 2, as only minor differences are noted.

In Fig. 2, it can be seen that the addition of a very small amount of H_2O reduces appreciably the steady-stage catalytic activity of ZS8(823)723 (curve 2). The activity declines sharply when higher fractions of the sample surface are exposed to water, and for nominal water coverages of $\approx$75% the catalytic activity towards *n*-butane isomerization is virtually suppressed. Therefore, an efficient dehydration of the ZrO_2/SO_4 catalyst turns out to be vital for best catalytic activity, in contrast with recent theoretical results (9), according to which superacidity requires the presence of residual water molecules in the system. The importance of the dehydration stage is confirmed by comparing the normalized activity at steady state of the ZS8(823)723 sample (7.8×10^{-6} mol h^{-1} m^{-2}) with that of ZS8(823)873 (10.4×10^{-6} mol h^{-1} m^{-2}), i.e., of a sample in which the activation/dehydration temperature is higher than that of the initial calcination. The steady-state activity of the ZS8(823)873 sample, made homogeneous to that of ZS8(823)723 by taking into account the different surface area, is represented by the broken-line trace in Fig. 2: it is seen that, despite a slightly lower concentration of sulfates (as reported in the experimental section), the catalytic activity of ZS8(823)873, a more dehydrated system, is higher than that of ZS8(823)723.

3.2. *Surface Sulfates*

Figure 3 reports the IR spectra in the vibrational region of surface sulfates relative to the ZS8(823) system after the vacuum activation at T_2 = 723 K (curve 1), and after the *in situ* addition of successive doses of water vapour (curves 2–5).

As it was pointed out by other authors (10), sulfate groups at the surface of the system isolated in a medium-high dehydration state possess a high covalent character. In fact, their spectra are comparable to those of organic sulfonates and sulfates (11). The background spectrum of ZS8(823)723 (trace 1 of Fig. 3) is characterized by:

(i) a strong and probably complex band centered at high frequency ($\nu \geq 1370$ cm^{-1}), due to the $\nu_{S=O}$ mode of surface $(ZrO)_3S{=}O$ species, as postulated by Bensitel *et al.* [10], and/or to the asymmetric O=S=O stretching mode of $(ZrO)_2SO_2$ species;

(ii) a broad unresolved band, centered at $\approx$1200 cm^{-1}, ascribed to the symmetric O=S=O stretching mode of some $(Zr)_2SO_2$ species, whose asymmetric mode lies in the unresolved high frequency envelope;

(iii) a broad and partially resolved band at $\approx$1000–1050 cm^{-1}, due to the ν_{S-O} stretching mode(s) of all surface sulfates. The highly covalent configuration of surface sulfates, typical of medium-high dehydration stages, is hereafter designated as C_1.

The high ν band of sulfates in configuration C_1 has a complex nature, and is most likely made up of several slightly different components. These correspond to sulfates of different structure and/or located in different crystallographic configurations, as observed in the case of better crystallized (monoclinic) ZrO_2/SO_4 systems (3); the various components cannot be resolved in the case of a disordered high-area (tetragonal) ZrO_2/SO_4 system like the present one.

In this medium-high dehydration stage of ZS8(823)723, there is no residual molecular (undissociated) water (no bands in the $\approx$1650 cm^{-1} range). The OH spectrum, shown by curve 1 of the inset to Fig. 3, is made up of a weak

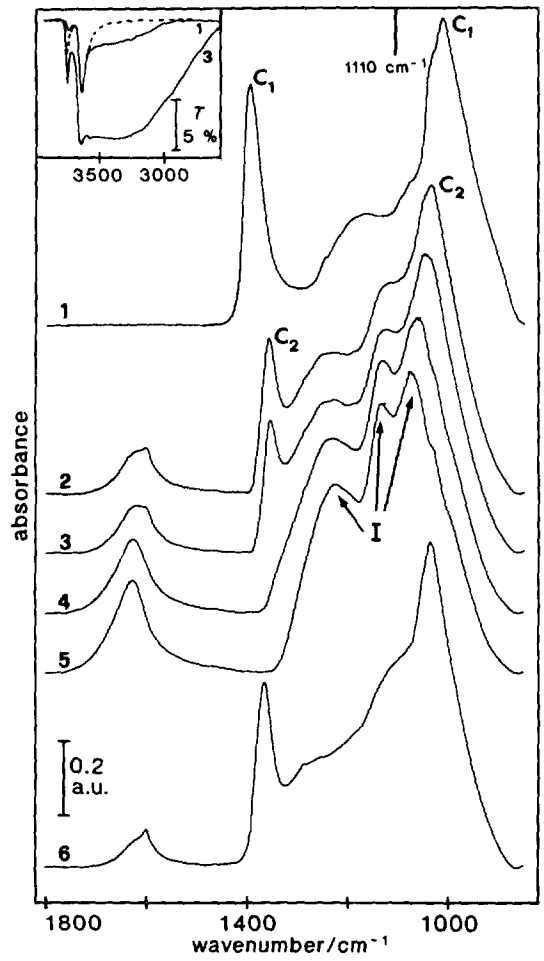

FIG. 3. Absorbance IR spectra of the ZS8(823) sample in the HOH deformation and S/O stretching region: (1) ZS8(823)723; (2–5) spectra run after the allowance of (gradually) increasing doses of H_2O, until reaching complete rehydration; (6) spectrum obtained by outgassing at 423 K the sample of curve 5 (i.e., after partial activation of a completely rehydrated material). *Inset*: Transmittance IR spectra in the OH stretching region: (1) ZS8(823)723. The broken-line trace shows the spectral profile of non sulfated ZrO_2 activated at 723 K. (3) Spectrum run after the allowance of the first two doses of water.

residual free OH component at ≈3765 cm^{-1}, of a relatively strong free OH component at ≈3665 cm^{-1}, and of a weak and broadish component at 3500–3000 cm^{-1}, due to OH groups involved in weak perturbations of the H-bonding type. The latter OH component is usually not observed on pure ZrO_2 isolated in a comparable dehydration stage, as shown by the dotted trace in the inset to Fig. 3, and could be due to a small residual amount of acidic OH groups. The latter could be responsible for a weak residual Brønsted acidity of the ZS8(823)723 system, which will be discussed below.

When water vapour is dosed onto ZS8(823)723, the spectrum of surface sulfates becomes gradually modified, and at least two stages can be distinguished:

(i) The strong high frequency $\nu_{S=O}$ mode is first shifted downwards of some 30 cm^{-1} (see the band at ≈1370 cm^{-1} in curves 2–3 of Fig. 3). This indicates the transformation of some of the surface sulfates with configuration C_1 into sulfates with a still basically covalent form, but less strongly so; this covalent configuration is hereafter designated as C_2. Meanwhile, the intense ν_{S-O} mode at ≈1000-1050 cm^{-1} moves upwards slightly (a decreased splitting of the two S–O vibrations is consistent with a decrease of the covalency), and new broadish bands start appearing at ≈1280 and ≈1130 cm^{-1}. New complex bands (to be discussed in more detail elsewhere; see curve 3 in the inset to fig. 3) appear in the 3800–2500 cm^{-1} ν_{OH} region, while a complex δ_{HOH} band, due to undissociated water molecules, is formed in the 1700–1600 cm^{-1} interval.

These early stages of water adsorption occur without the building up of a detectable equilibrium water pressure.

(ii) Under the effect of higher water doses, also the sulfates in configuration C_2 ($\nu_{S=O}$ mode at ≈1370 cm^{-1}) are eliminated (see curves 4–5 of Fig. 3). Meanwhile, the bands at ≈1280 and ≈1130 cm^{-1} become dominant (the former band gradually shifts down to ≈1240 cm^{-1}), the ν_{S-O} mode shifts further to higher wavenumbers, and a weak shoulder appears at ≈1000 cm^{-1}. It is recalled that a complex SO_4 spectrum with three resolved components of the ν_3 mode (≈1280, ≈1130, and ≈1070 cm^{-1}) and a weakly active ν_1 mode (≈980 cm^{-1}) is typical of sulfato complexes in a bidentate configuration with symmetry lower than C_{3v} (12). Also, three components of the ν_3 mode, resolved at ≈1215, ≈1150, and ≈1085 cm^{-1}, are observed in anhydrous inorganic sulfates (e.g., see the case of $CuSO_4$, symmetry C_{2v} (13)), in which the removal of solvating water brings about the direct coordination of the SO_4 ion to the metal ion(s). The surface sulfates of the ZrO_2/SO_4 system, brought by hydration into a more ionic configuration comparable to that of inorganic sulfato complexes and/or of anhydrous inorganic sulfates, are hereafter designated as I.

This second stage of the rehydration process occurs with the building up of an appreciable equilibrium water pressure. In this stage, a fair amount of coordinated and/or physisorbed water is present at the surface, as revealed by the strong broad and unresolved δ_{HOH} band at ≈1630 cm^{-1}. Further doses of water, bound to increase only the physisorbed component, will further increase intensity and breadth of the δ_{HOH} band at ≈1640 cm^{-1}, and will further increase the ionicity of the SO_4 ligands. The split components of the ν_3 mode will become closer to one another and ideally tend very slowly to the spectral position of the unresolved F_2 mode of SO_4 groups of T_d symme-

try, typical of hydrated inorganic sulfates (13) (see the mark at ≈1110 cm^{-1} in Fig. 3).

The isomerization reaction was shown in the previous section to proceed rapidly at 423 K on the ZS8(823)723 catalyst. In order to simulate the actual situation produced at the surface of the working catalyst by the injection at 423 K of large doses of water, the rehydrated sample was outgassed at 423 K. The relevant IR spectrum is shown as curve 6 in Fig. 3. Most of the effects produced at ambient temperature by the last large doses of water are reversed, and the spectral features become similar to those of a partly rehydrated system on which the sulfates are partly in configuration I and mostly in configuration C_2. In fact, the spectrum of sulfates of curve 6 is very similar to that of curve 2. In this early dehydration stage, also the spectrum of surface water species becomes very similar to that corresponding to the first steps of water adsorption. In fact, the δ_{HOH} band exhibits again the complex shape it had during the first rehydration stages, with a partly resolved sharp component at ≈1600 cm^{-1} that is most likely ascribable to $[H_3O]^+$ ions, present in this stage of rehydration together with abundant surface sulfates in C_2 and/or I configuration.

As the rehydration was shown above to decrease the catalytic activity of ZS8(823)723 in the isomerization process, it is inferred that surface sulfates in I (ionic) or in C_2 (covalent) configuration, and the corresponding surface acidity, do *not* induce superacidity and catalytic activity in the ZrO_2/SO_4 system. This datum is in contrast with the conclusion of Babou *et al.* (9).

3.3. Surface Acidity

The total acidity of the ZS8(823)723 systems was tested by ambient temperature adsorption/desorption of pyridine (py). In fact it is known that py uptake at ≈300 K approaches closely the complete surface coverage, and can distinguish between Lewis and Brønsted acidity (14).

The strongest component of the Lewis acidity was tested by ambient temperature adsorption of CO. In fact on d^0 metal oxides CO uptake at ≈300 K is fairly low, as it σ-coordinates only onto the most uncoordinated (cus) surface cationic sites (e.g., see Ref. (15)).

Curve 1 of Fig. 4 is relative to py uptake onto ZS8(823)723. It shows that, after activation, at the surface of the catalyst there is a fair amount of Lewis acidic sites (monitored by the 8*b* [py–L] band at ≈1580 cm^{-1}, and by the 19*b* [py–L] band at ≈1445 cm^{-1}). The amount of Brønsted acidic sites is quite small (monitored by the dashed-area 19*b* band of [py–B] at ≈1540 cm^{-1}, and by the low relative intensity of the 19*a* py band at ≈1490 cm^{-1}, common to [py–L] and [py–B], with respect to the [py–L] band at ≈1445 cm^{-1}).

After exhaustive rehydration of the ZS8(823)723 catalyst and a prolonged *in situ* evacuation in the IR beam of the excess water (i.e., in a situation similar to that obtainable by evacuation at 423 K), the adsorption/evacuation of py at ambient temperature yields the spectrum shown by curve 2 of Fig. 4. It can be noted that the relative amount of [py–L] and [py–B] species has been severely modified. In fact, the latter species is now far more abundant. Note that, after evacuating at ≈423 K the rehydrated ZS8(823) material, py uptake would yield a very slightly modified situation (if at all): the analytical bands of [py–B] reach the same level of curve 2 of Fig. 4, and the bands of [py–L] are somewhat stronger than in curve 2 of Fig. 4, due to the removal on evacuation of most of the residual coordinated undissociated water, replaced by the coordination of some more [py–L]. (After sample evacuation at beam temperature, the shallow band due to the δ_{HOH} mode of water that remains coordinated also in the presence of adsorbed py is indicated in curve 2 of Fig. 4 by an arrow).

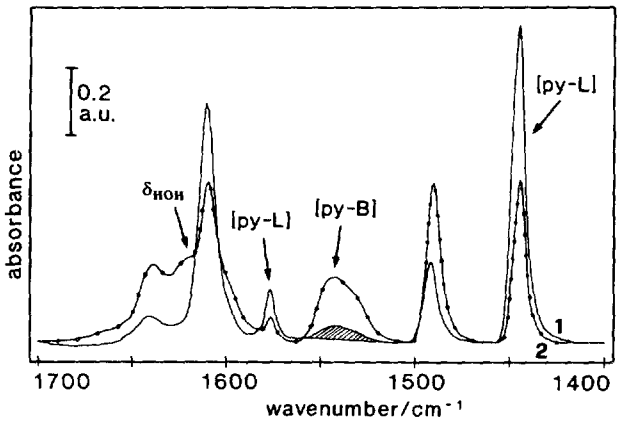

FIG. 4. Absorbance IR spectra of pyridine (py) adsorbed at ≈300 K on ZS8(823) samples, and run in the analytical region of the 8*a*–8*b* and 19*a*–19*b* py ring modes. (1) Solid-line trace: 8 Torr py was first adsorbed, and the excess py was then evacuated at room temperature (RT). (2) Dotted-line trace: 8 Torr py was adsorbed at ≈300 K (and the excess py desorbed at the same temperature) on the ZS8(823)723 sample fully rehydrated, and then evacuated at beam temperature (≈345 K).

It is thus deduced that:

(i) The rehydration of ZS8(823)723 reduces drastically the overall surface concentration of aprotic Lewis acidic sites, as expected, and some of the Lewis centres are converted into protonic Brønsted centres. This partial transformation of [py–B] species into [py–L] species was postulated also by Arata (1), although in the case of the SO_4/ZrO_2 systems dealt with by Arata the spectral Lewis–Brønsted changes were less evident and much less abundant than in the present case.

If the Brønsted centres are OH groups in the coordination sphere of (some of) the surface sulfates, the sulfates

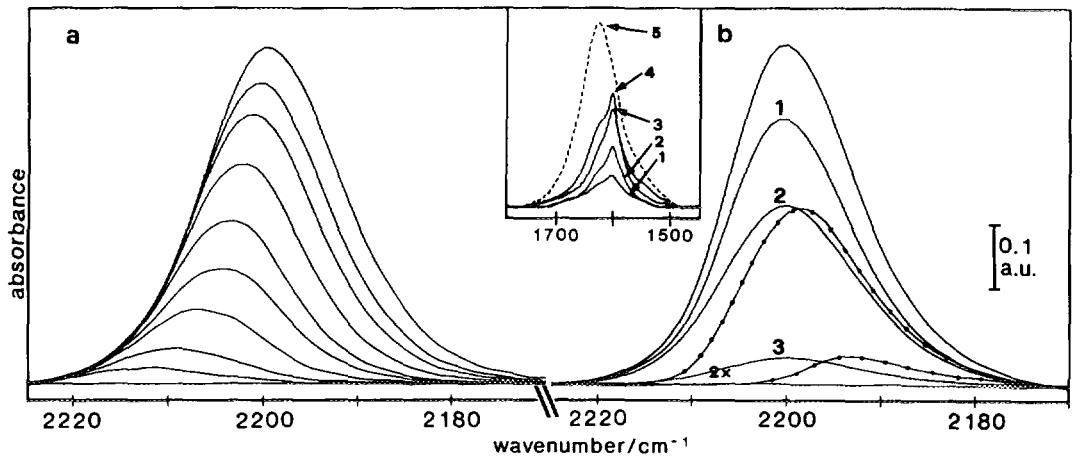

FIG. 5. Absorbance spectral patterns of CO uptake at ≈300 K onto the ZS8(823) sample. (a) CO adsorption isotherm onto ZS8(823)723 (P_{CO} in the 1×10^{-1}–1×10^{2} Torr range). (b) adsorption of 100 Torr CO onto a ZS8(823) sample, isolated in different hydration/dehydration stages. Top solid-line curve: ZS8(823)723; (1–3) the same ZS8(823)723 sample after the allowance of small increasing H_2O doses (curve 3 underwent a twofold ordinate scale expansion). Bottom solid-line curve: CO was allowed onto the ZS8(823)723 sample exposed to ≈1 Torr H_2O (the sample was so abundantly rehydrated, but not fully rehydrated yet). Bottom dotted-line curve: CO was allowed onto a fully rehydrated ZS8(823) sample, after dehydration at T_2 = 373 K. Top dotted-line curve: CO uptake, after dehydration at T_2 = 473 K of a fully rehydrated ZS8(823) sample. *Inset* to (b): absorbance IR spectra in the δ_{HOH} mode region of the ZS8(823) sample: (1–3) after the allowance onto ZS8(823)773 of small H_2O doses, corresponding to the decreasing activity towards CO shown in (b); (4) after dehydration at T_2 = 373 K of a fully rehydrated ZS8(823) sample. This curve corresponds to the residual activity towards CO shown in (b) by the bottom dotted curve; (5, broken-line trace) the fully rehydrated ZS8(823) sample.

bearing the acidic OH groups must be mostly in the covalent form C_2 and/or in the ionic form I.

(ii) If the acidic centres giving the activated catalyst its superacid properties do belong to the family of Brønsted protonic sites, as postulated by some authors (2), these must be only a minor amount of OH groups free from H-bonding and carried by covalent sulfates of the C_1 family. Opposite to that, the vast majority of acidic OH groups, that in proper hydration conditions are in a hydrated form and are carried by C_2 and/or I sulfates, are catalytically not active.

The effect of rehydration on the strong Lewis acidity of ZS8(823)723, revealed by CO adsorption at 300 K, is illustrated by Fig. 5. Figure 5a shows that, on the catalyst activated at 723 K, CO uptake at ≈300 K yields a broad and probably complex band in the 2230–2180 cm^{-1} interval. CO adsorption is reversible, confirming a weak interaction of the σ-dative type. The frequency of the band maximum decreases with increasing CO coverage, indicating some intrinsic and/or induced heterogeneity of the adsorbing sites. It is recalled that both types of heterogeneity are normally observed at the surface of microcrystalline monoclinic ZrO_2 (15) and of monoclinic ZrO_2/SO_4 (16).

Figure 5b shows that the allowance of the very first doses of water vapour onto ZS8(823)723 has a fast detrimental effect on the catalyst activity towards CO. The band intensity declines fast, while the band breadth and frequency remain virtually unchanged, indicating that the distribution of intrinsic sites heterogeneity and the acidic strength of the residual strong Lewis sites remain the same. Note that the sites strength distributions during rehydration and dehydration do not coincide. In fact, the spectral pattern in Fig. 5b shows that comparable stages of CO uptake can be reached during the dehydration (dotted traces) and the rehydration process of ZS8(823) (solid-line traces), but the ν_{CO} stretching frequencies do not coincide.

The inset to Fig. 5b shows the δ_{HOH} band that is built up during the water allowances that lead to complete disappearance of the adsorptive activity towards CO (curves 1–3). The δ_{HOH} band labeled 3 exhibits the resolved shape typical of the first rehydration steps discussed above, and is similar to the spectrum corresponding to evacuation at ≈323 K (curve 4) of a fully rehydrated system (full rehydration is represented by the broken-line spectrum 5). In particular, it can be noted that the activity towards CO at 300 K is virtually extinguished when the δ_{HOH} band reaches the intensity of curve 3. The intensity is almost equivalent to (actually, slightly weaker than) the δ_{HOH} band 4, which corresponds to the complete conversion of C_1 sulfates into C_2 and I sulfates, and to the complete suppression of the catalytic activity of the ZS8(823)723 system in the isomerization reaction.

It is thus deduced that the early steps of rehydration, that bring about the conversion of some Lewis sites into

Brønsted ones, correspond to the selective suppression of the strongest fraction of Lewis sites, active towards CO at 300 K. As the early steps of rehydration also extinguish the catalytic activity of ZS8(823), the presence of the strongest fraction of Lewis sites is strictly related, and most likely necessary, to the catalytic activity. On the basis of CO adsorption and H_2O adsorption/desorption spectral data, the amounts of strong Lewis sites and of catalytically active Lewis sites are virtually equivalent.

The actual concentration and strength of the Lewis acidic sites that can chemisorb CO at ≈300 K, that are selectively poisoned in the first stages of rehydration, and that are probably involved in the isomerization reaction is presently being tested volumetrically and calorimetrically.

4. CONCLUSIONS

The data presented here show that the hydration/dehydration stage reached by the ZS8(823) system is most sensitively monitored by the structural configuration of surface sulfates. The catalytic activity of the ZS8(823) system in the *n*-butane isomerization reaction is strictly related to the dehydration stage.

The present data do not prove that protonic Brønsted acidic centres are not active at all in the catalytic isomerisation process. In fact, small amounts of protonic sites remain at all dehydration stages, up to the temperatures at which surface sulfates start being thermally decomposed (17). Certainly, our results show that a dependence of the catalytic activity of this ZrO_2/SO_4 system on the overall amount of Brønsted acid centres is unlikely.

The catalytic activity of the ZS8(823) system is maximum when the surface sulfates are in a highly covalent configuration, and at the surface is maximum the amount of strong Lewis acidity, whereas that of Brønsted acidity is minimum.

These data are thought to represent a progress in the identification of the sites catalytically active. Still, more data are necessary, concerning, for instance, the number of active sites and the selective poisoning of the catalytic activity by molecules other than water, before one can try a schematic representation of the sites responsible for *n*-butane isomerization at the surface of SO_4/ZrO_2 systems.

ACKNOWLEDGMENTS

This work was partly supported by the C.N.R. (Rome), Progetto Finalizzato Materiali Speciali. The authors are indebted to Professor C. Sarzanini (University of Turin), who performed the analysis of sulfates.

REFERENCES

1. Arata, K., *Adv. Catal.* **37,** 165 (1990).
2. Nascimento, P., Akratopoulou, C., Oszgyan, M., Coudurier, G., Travers, C., Joly, J. F., and Vedrine, J. C., *in* "Proceedings 10th International Congress on Catalysis, Budapest, 1992" (L. Guzci, F. Solymosi and P. Tetenyi, Eds.), Vol. B, p. 1185. Akadémiai Kiadò, Budapest, 1993.
3. Morterra, C., Cerrato, G., Emanuel, C., and Bolis, V., *J. Catal.* **142,** 349 (1993).
4. Tanabe, K., Hattori, H., and Yamaguchi, T., *Crit. Rev. Surf. Chem.* **1,** 1 (1990).
5. Parera, J. M., *Catal. Today* **15,** 481 (1992).
6. Wen, M. Y., Wender, I., and Tierney, J. W., *Energy and Fuel* **4,** 372 (1990).
7. Morterra, C., Bolis, V., Cerrato, G., Pinna, F., Signoretto, M., and Strukul, G., *Europacat-I, Montpelier, September 12–17, 1993,* paper I-77.
8. Chen, F. R., Coudurier, G., Joly, J.-F., and Vedrine, J. C., *J. Catal.* **143,** 616 (1993).
9. Babou, F., Bigot, B., and Sautet, P., *J. Phys. Chem.* **97,** 11501 (1993).
10. Bensitel, M., Saur, O., Lavalley, J. C., and Morrow, B. A., *Mater. Chem. Phys.* **19,** 147 (1988).
11. Bellamy, L. J., "The Infrared Spectra of Complex Molecules. Vol. 2. Advances in Infrared Group Frequencies," p. 225. Chapman and Hall, London, 1980.
12. Nakamoto, K. "Infrared and Raman Spectra of Inorganic and Coordination Compounds," 4th ed., p. 249. Wiley, New York, 1986.
13. Ferraro, J. R., and Walker, A., *J. Chem. Phys.* **42,** 1278 (1965).
14. Parry, E. P., *J. Catal.* **2,** 371 (1963).
15. Morterra, C., Orio, L., and Emanuel, C., *J. Chem. Soc. Faraday Trans.* **86,** 3003 (1990).
16. Morterra, C., Bolis, V., Cerrato, G., and Magnacca, G., *Surf. Sci.,* **307–308,** 1206 (1994).
17. Morterra, C., Bolis, V., and Cerrato, G., *Catal. Today* **17,** 505 (1993).